Accepted article. International Conference on Robotics and Automation.

Tactile sensing based on fingertip suction flow for submerged dexterous manipulation

Philippe Nadeau, Michael Abbott, Dominic Melville and Hannah S. Stuart*

***Abstract*— The ocean is a harsh and unstructured environment for robotic systems; high ambient pressures, saltwater corrosion and low-light conditions demand machines with robust electrical and mechanical parts that are able to sense and respond to the environment. Prior work shows that the addition of gentle suction flow to the hands of underwater robots can aid in the handling of objects during mobile manipulation tasks. The current paper explores using this suction flow mechanism as a new modality for tactile sensing; by monitoring orifice occlusion we can get a sense of how objects make contact in the hand. The electronics required for this sensor can be located remotely from the hand and the signal is insensitive to large changes in ambient pressure associated with diving depth. In this study, suction is applied to the fingertips of a two-fingered compliant gripper and suction-based tactile sensing is monitored while an object is pulled out of a pinch grasp. As a proof of concept, a recurrent neural network model was trained to predict external force trends using only the suction signals. This tactile sensing modality holds the potential to enable automated robotic behaviors or to provide operators of remotely operated vehicles with additional feedback in a robust fashion suitable for ocean deployment.**

I. Introduction

Hands capable of performing grasping and manipulation underwater can enable robotic platforms to better address challenging field applications, such as ocean exploration [1]. A sense of touch, via tactile sensors, supports the implementation of autonomous grasp reflexes, manipulation primitives, physical probing of the environment and haptic feedback to teleoperators. Sensing physical interaction forces is especially useful in the ocean, where vision is easily diminished by darkness or silty waters and objects may be fragile. For example, France's Department of Underwater and Submarine Archaeological Research asserts that this sense of touch will be "the key feature of future handling devices" [2].

The ocean is a harsh, unstructured environment for robotic systems. Mechanical compliance is a useful way to create robust grippers for highly unstructured environments, described in a number of reviews, chapters and research articles such as [3]–[6] which detail a variety of underactuated and soft designs. The contact-rich nature of these compliant hands means that their behavior is susceptible to subtle changes in contact conditions; these conditions can be measured directly by tactile sensors in the skin. Yet, the inclusion of tactile sensors into compliant hands is a challenge due to practical limitations – there is finite space in the fingers for embedding electrical components and wires get fatigued as the fingers flex repetitively.

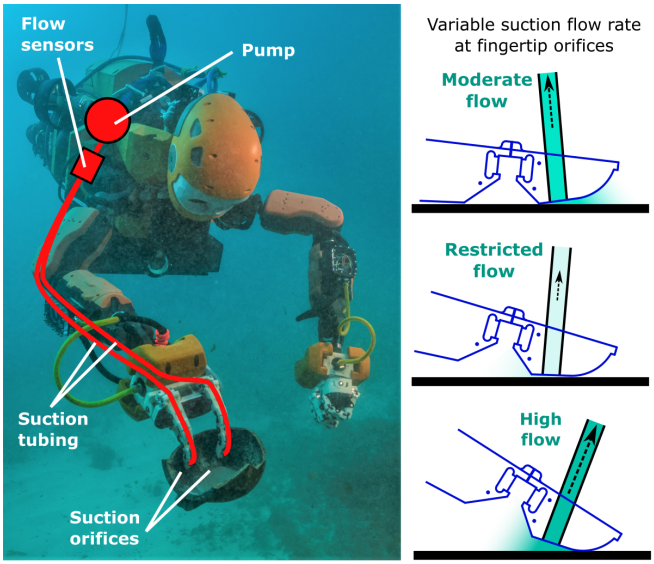

Fig. 1. The addition of suction flow can improve underwater grasping. Pumps and sensitive measurement electronics can be incorporated remotely to the hand, proximal to the arm (left, photo credit: Frederic Osada and Teddy Sequin, DRASSM/Stanford University). The flow rate drawn through the orifice changes with contact orientation, as the fingertip rolls or slips across a smooth flat plate (right).

In this work, we introduce a new method of tactile sensing using gentle suction flow at the fingertips of a compliant hand, as in Fig. 1, that is convenient to incorporate into underwater robots. One main benefit of this solution is that pumps and sensitive electronics can be located remotely from the hand, protected on the robotic base proximal to the arms.

Section II reviews the state of the art of hands and tactile sensing for marine operations, including the use of suction flow to improve grasping under water. The design of the suction flow tactile sensor is described in Section III, with special attention given to the flow rate measurement system and the compliance and shape of the skin at the fingertips of the hand. Suction flow tactile sensing produces a meaningful yet complex signal. As a proof-of-concept, we use data-driven machine learning methods to process data from a set of grasping experiments during a pipe handling scenario, described in Section IV. The results presented in Section V show that suction flow tactile sensing is capable of providing an estimate of the grasp pullout force trends, which may have importance for certain manipulation tasks as discussed

P. Nadeau is with the Dept. of Systems Engineering, École de Technologie Supérieure, Montréal, Québec, Canada. He completed this work as a visiting student at the University of California Berkeley.

M. Abbott, D. Melville and H.S. Stuart are with the Dept. of Mechanical Engineering, University of California Berkeley, Berkeley, CA, USA.

* Corresponding author (email: hstuart@berkeley.edu)

in Section VI. We conclude in Section VII with future steps.

II. Related Work

A. Hands for Ocean Operation

A number of robotic hands and grippers are specialized for marine applications, including [7]–[11]. Solutions range from rigid claw-type designs produced for industry, e.g., [12], to extremely gentle and compliant hands, e.g., for grasping onto jellyfish [13]. Suction cups are sometimes utilized in gripping underwater, e.g., tagging marine mammals [14] or handling archaeological artifacts [15]. Previous research published in [16] shows that gentle suction flow at the fingertips of an underwater, multifinger hand enhances the reliability of grasping and holding a variety of objects through increased attractive forces and coefficients of friction, even when a suction seal is not completely achieved.

B. Tactile Sensing Underwater

In the ocean, tactile sensors must withstand large variations in ambient pressure associated with changes in depth and rough wear typical of unpredictable environments. There is a rich literature regarding the design of tactile sensors for robot manipulation summarized in reviews, e.g., [17], [18], and chapters, e.g., [19]. Groups that directly address large changes in hydrostatic pressure for subsea operation use dynamic sensors (e.g. PVDF film) [20], bulk-incompressible soft materials [21], [22], fluid-filled pressure-compensated cavities [23], or measure structural strain [24].

Suction flow was first mentioned as a potential means of measuring contact engagement in the discussion section of [25]. This tactile sensing modality does not require electronics to be included directly on the hand because flow can be measured anywhere along suction tube lines. Stuart et. al. observed that fingertip suction flow rate is a complex signal that varies with the details of the finger, object and manipulation behavior. To the authors' knowledge, the current work is the first demonstration of fingertip suction flow as a tactile sensor applied to submerged robotic manipulation.

C. Other sensitive fluid-flow systems

There are works which incorporate suction onto multifinger hands for operation in air, such as [26], [27]. Several warehouse robots have successfully used suction as an actuation mechanism in addition to a gripper to pick porous or smaller items, such as those developed for the Amazon Robotics Challenge (ARC) [28], [29]. The winning team of ARC's 2017 edition also incorporated suction sensing with the inclusion of a pressure switch that allowed them to detect when the vacuum seal was made or broken [29]. Other robotic systems, like wall-climbing robots equipped with suction cups, use pressure sensing for feedback when attaching and dettaching a vacuum foot [30], [31]. These applications typically treat suction pressure or flow as a binary engagement signal. Submersion in a denser and more viscous fluid – e.g., water – reduces the sensitivity of suction flow rate on sealing effects at the contact. Thus, contact suction flow rate is a more suitable analog signal under water compared with in-air applications.

III. Implementation

A. Suction flow monitoring

Flow sensing is implemented using a pressure gradient technique imposed by a flow resistor. A Venturi tube (entry diameter = 10 mm, throat diameter = 6 mm) is placed at the outlet of a centrifugal pump, shown in Fig. 2, and produces a pressure difference based on flow rate through the tube. One benefit of using a differential pressure transducer in this tactile sensor is that flow readings will be independent to changes in ambient pressure.

The relationship between pressure and flow rate in the Venturi tube can be expressed by the equation $Q = \sqrt{CP}$, where Q is the flow rate measured in m^3/s, P is the differential pressure $P_1 - P_2$ measured in Pa, and C is a constant determined by the Venturi tube diameters and fluid density. Given our parameters, $C \approx 1.84 \cdot 10^{-12}\ \mathrm{m}^7\mathrm{kg}^{-1}$. A differential pressure transducer (MPXV7025DP) measures the pressure drop between the entry and throat portions of the Venturi tube with a sensitivity of 90 mV/kPa. Due to the overall nonlinear relationship between pressure and flow rate, however, flow sensitivity ranges from 8.17 mV/LPM at the no-flow condition to 350 mV/LPM at pressure transducer saturation. The submerged centrifugal BLDC pumps (DC40-2470) used in this paper produce a maximum of 3.4 LPM when connected to the suction tubes and Venturi flow resistors in the complete system.

B. Considerations for integration with a hand

The unique sensitivities of contact suction flow tactile sensing influence its application to a hand. In this work, the hand mechanism, shown in Fig. 3(a), is comprised of two independently actuated fingers placed in opposition to enable pinch grasps. The design of the fingers is largely drawn from those used in the Ocean One hands, which are discussed in-depth in [8]. The fingers have three phalanges connected by soft flexures. Each finger is driven by a single tendon, and stainless steel springs across each joint act to maintain tendon

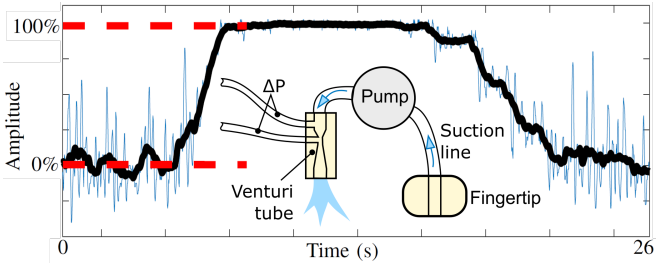

Fig. 2. Inset diagram of suction flow sensing hardware. A centrifugal pump pulls fluid through a suction orifice in the fingertip and pushes the fluid out through a Venturi tube flow sensor. A differential pressure transducer measures ΔP and outputs a DC voltage signal based on the pressure drop and related flow rate through the tube. The plotted raw suction flow signal, taken during a single clogging and unclogging sequence, is amplified and digitized (blue) and then filtered (black) before being used in later analysis. The suction engagement is expressed in terms of percentage where 0% means that there is no suction engagement with an object (i.e. maximum flow rate) while 100% means that the suction orifice is fully clogged (i.e. no flow).

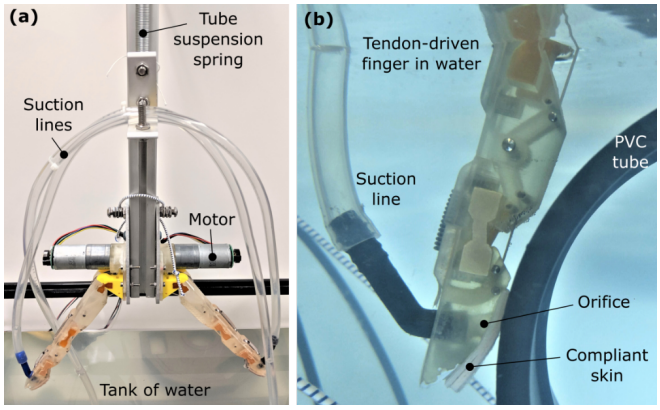

Fig. 3. (a) The hand in this work is made up of two independently actuated fingers. The suction lines are routed above the hand via a tube suspension spring to reduce the influence of tube flexing on finger motion. (b) Close-up image of fingertip shows key elements: a cylindrical test object (PVC tube), finger joint mechanism, compliant foam skin, orifice location and suction tube directing fluid towards the flow sensor.

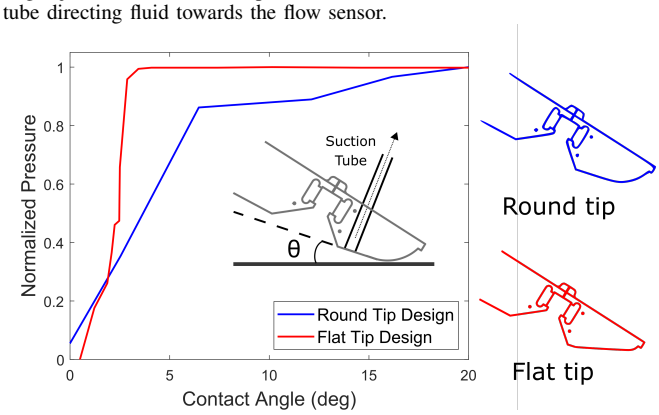

Fig. 4. The sensitivity of the suction flow sensor with respect to contact angle θ for two different fingertip geometries. A round tip design produces a more gradual response than with a flat tip design.

tension and define curing behavior throughout the travel of the finger. Suction orifices are located at the fingertips because (1) suction can meaningfully improve the strength of a pinch grasp and (2) even objects held in a wrap grasp are likely to interact with the fingertips if they are pulled out of the hand to grasp failure. Arrays of smaller suction orifices could be installed across the entire hand, providing more spatial resolution or area of detection. It should be noted that coupling multiple orifices to a single flow sensor will reduce the magnitude of contact measurand signal on any single orifice. This is why, in this work, a dedicated pump is applied to each individual suction orifice.

The suction flow rate is sensitive to small gaps between the orifice and object surface, with distances up to ≈1 mm [16]. Details of fingertip geometry can alter the response of the sensor with respect to contact angle. An initial experiment compares two rigid fingertip profiles as contact angle changes, the results of which are shown in Fig. 4. A contact point further away from the orifice (i.e. towards the distal edge of the phalanx) produces a larger change in distance for a given contact angle. Similarly, rounded portions near

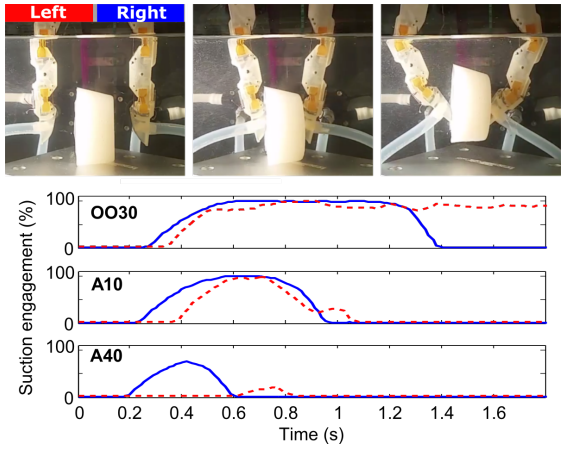

Fig. 5. Two opposed fingers pinch rubber or plastic objects of varying compliance. Suction engagement is maintained for considerably longer for the softer rubber (Shore OO30) than the hard plastic (Shore A40).

the orifice result in a more gradual response. As we wish to evaluate this sensor over a wide range of contact angles, a rounded fingertip geometry was selected for all experiments in this work, shown in Fig. 3(b).

Contact compliance also improves suction engagement over a wider range of contact angles. A soft skin will act like a gasket, while a rigid fingertip will exhibit a sharper flow response to variations in orifice misalignment with the object. This idea is demonstrated in Fig. 5, while palpating rubber blocks using the 2-finger hand; the most compliant object produces the most suction engagement throughout the manipulation, while the most rigid object does not completely clog either fingertip orifice. In order to achieve repeatable results during the experiments described in Sec. IV while handling rigid objects, a foam skin was placed over the fingertip pad. The soft skin is comprised of one layer of double-sided urethane foam tape and an outer layer of 1/16" closed-cell polyethylene foam, pictured in Fig. 3(b). A hole in the foam and tape layers allows for unobstructed fluid flow through the suction orifice.

In the current experimental implementation, the weight and flexing of the suction line impacts the motion of the finger. Deviation of the tubing out of the plane of finger motion causes the compliant joints to twist. Because the suction flow sensor is highly sensitive to contact angle, this misalignment of the fingertip alters the suction engagement during grasping. As seen in Fig. 3(a), a tube suspension spring system is used to limit this effect. Careful and consistent integration of the suction lines is especially important for using this modality as a tactile sensor in soft robot hands. Also, the aspiration of dirt or other matter is a concern with suction flow as clogging events could lead to detection of false-positive manipulation events. Disabling or reversing the flow could be used to mitigate this issue, and will be examined in future work.

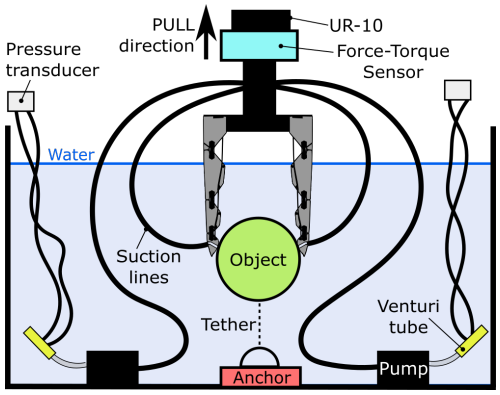

Fig. 6. Schematic diagram of experimental setup for grasping trials. The hand is moved upward by a UR-10 robot arm while a Robotiq FT-300 force-torque sensor measures forces at the wrist. The studied object is held down by an anchored string or extension spring. The chosen location of the pumps and the position of the suction lines reduces deviation of the tubing out of the plane of finger motion but can be changed as long they do not impede finger movement.

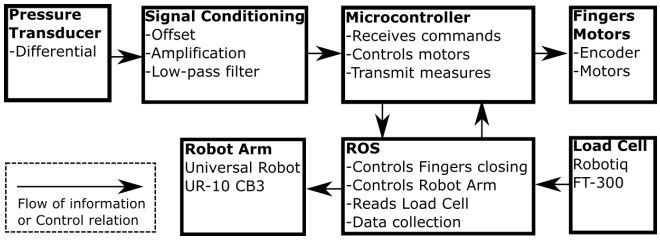

Fig. 7. The control and monitoring environment was centered around the Robot Operating System (ROS) and allowed an important level of automation in the data collection process.

IV. Experimental Methods

In order to characterize the utility of the suction flow sensor for robotic handling, a series of grasp trials were performed to test the sensor in underwater conditions.

A. Experimental setup

A diagram of the underwater test setup is shown in Fig. 6. The grasping trials took place in a 70 L water tank filled with enough water such that the fingers were submerged throughout the grasping experiments. The robotic hand described in Sec. III was attached to a Universal Robots UR10 robotic arm to facilitate hand motions. Water was pulled through orifices in the fingertips, through a set of tubes, and out through the Venturi tubes. A set of objects for grasping trials are placed in the tank; a small piece of foam inside each object makes it approximately neutrally buoyant. Two suction cups at the bottom of the water tank anchor the object in the grasping plane and extension springs attached to the test object and the suction cups prevent the object from getting pulled completely out of the tank during grasping trials. The Robot Operating System (ROS) was used to automate the experimental processes as shown in Fig. 7. A Robotiq FT-300 force and torque sensor measured the loads acting on the hand mechanism during the experimental trials. Data regarding gripper depth, suction engagement level, and forces acting on the hand mechanism were logged at a rate of 70 Hz.

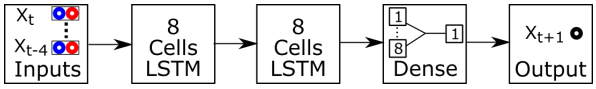

Fig. 8. Architecture of the standard LSTM-based neural network.

B. Experimental procedure

For each trial, the hand was lowered down to a constant depth, and the fingers were closed around the test object until the suction engagement level at the fingertips was above a given threshold, measured by the suction flow tactile sensor. The gripper was then raised several centimeters vertically upward, extending a spring attached to the test object, eventually causing the object to be pulled out of the hand. Two modes of operation were used when pulling on the object: (1) raising the object at a continuous speed and (2) raising the object through a series or short upward arm movements. After grasp failure, the gripper was then lowered back to its initial state for further trials.

Two PVC tubes with diameters of 4 and 6 inches were used as test objects, specifically selected because the grip on larger objects is more reliant upon suction forces [16]. A total of 80 independent experimental grasping trials were performed, 60 of which were conducted using the 6 in. diameter pipe and 20 were conducted using the 4 in. diameter pipe. The trials using the large tube were done in a smooth vertical motion while the trials with the smaller pipe were executed in discontinuous motions. The trials were equally divided into five initial levels of suction engagement (20%, 30%, 40%, 50% and 60%) across all modes and object sizes.

C. Predictive model generation

In order to investigate whether the signals from the flow sensors could be a useful predictor of the pullout force of a grasp, a recurrent neural network (RNN) was used, whose architecture is summarized in Fig. 8. This algorithm has shown a high level of performance for highly volatile time-series prediction tasks where it outperformed autoregressive integrated moving average (ARIMA) and Support Vector Machine Regression (SVR) algorithms by a significant margin [32] [33]. The Keras [34] and Tensorflow [35] frameworks were used to train the RNN with a truncated back-propagation through time. A sliding window of five time steps was used to predict the next value of the output by using standard long short-term memory (LSTM) layers. The input was then fed to a sequential stack made of a first LSTM layer of eight memory cells followed by a second similar layer and finally followed by a densely-connected layer. A manual hyper-parameters search was conducted on the validation set, and the mean squared error metric was used with the Adam [36] optimizer.

The RNN model was trained using only the smooth/large dataset, using suction data alone as an input. The training and validation sets were comprised of 47% and 12% respectively

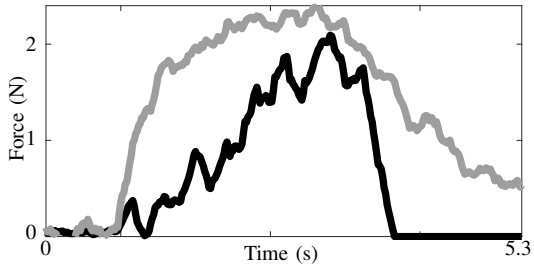

Fig. 9. Typical evolution of the reaction force over time for a smooth motion trial (grey) with a large tube and a discontinuous motion trial (black) with a smaller tube.

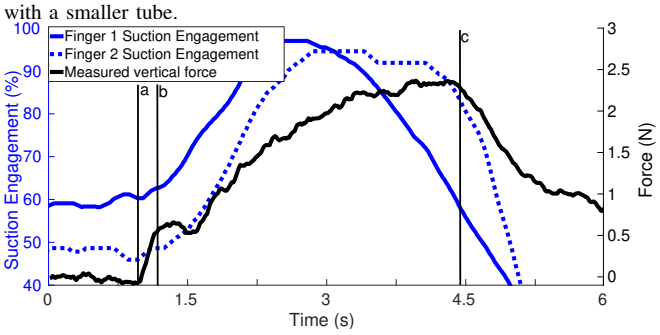

Fig. 10. A typical evolution of the vertical force (black) and of the suction engagement (blue). Initially (a), no vertical force is exerted and the suction is moderately engaged and constant. As the robot arm pulls the object, the measured force is increased (b) but the suction engagement remains relatively unchanged. Both the force and the engagement then grow up to their respective maximum before reaching a point where they decrease rapidly (c).

TABLE I

SUMMARY OF TRIALS

Mode	Smooth	Discontinuous
Object	Large (⌀6 in.)	Small (⌀4 in.)
Qty. of trials[1]	60	20
Max. Force Mean	1.82 N	1.34 N
Max. Force Std. Dev.	0.46 N	0.41 N

[1]: Each category was equally divided into 20%, 30%, 40%, 50% and 60% suction engagement thresholds.

of the smooth/large data. The trained RNN model was then tested on 25 smooth/large trials and 20 discontinuous/small trials. For each test, the mean absolute error (MAE) between the predicted and measured force values are reported.

V. RESULTS

A summary of the 80 grasping trials is presented in Table I; for each trial, the maximum force resisted by the grasp prior to failure was found from the gathered data. The tubes and skin provide a relatively low amount of contact friction, which results in low maximum pullout forces. The standard deviation is 25% and 31% of the mean for the smooth/large and discontinuous/small trials respectively, indicating that this experimental system contains significant variability representative of real-world grasping. Fig. 9 shows typical continuous/large and discontinuous/small vertical force over time during the pulling phase of the trials – the shape of the force profiles of these two experimental conditions differ significantly.

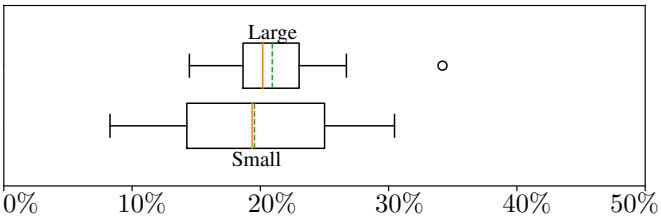

Fig. 11. Distribution of the mean absolute error (MAE) of the predicted force for both objects using the model trained on the large object. The mean (green, dashed vertical line) of the MAE is 21% for the large tube and 20% for the smaller one. Whiskers have a maximal length of 1.5 times the interquartile range.

As demonstrated with a single pulling trial under continuous/large-tube conditions in Fig. 10, there is an apparent correlation between the evolution of fingertip suction flow rates and the external force acting on the object. The suction engagement sensors start at an initial set-point. As the object starts to be pulled vertically, more of the suction orifice is occluded by the contact, resulting in more suction engagement. The suction engagement of the two fingers appears to peak at slightly different times during the maneuver. By the time the grasp starts to fail, defined here as a decrease in the pulling force, both suction engagement sensors are already decreasing rapidly, which indicates that the object is rolling/sliding past the fingertips. While the qualitative correlation between suction sensing and pullout force are apparent in this single trial, significant variability between different grasp trials creates challenges for defining a single closed-form prediction based solely on suction flow.

The performance of the RNN model, produced using the procedure discussed in Sec. IV-C, is shown in Fig. 11. The model achieved an MAE of 21% for the continuous/large trials and 20% for the discontinuous/small trials. Similar performance under both conditions indicates that the trained model is robust to slight changes in object size and pulling behavior. Yet, the discontinuous/small outcomes are more varied, which is expected because the model was not exposed to this condition. The data from two trials are shown as examples in Fig. 12. In cases with lower MAE, this preliminary model appears to capture the shape of the force profile.

VI. DISCUSSION

Suction flow sensing is able to provide a measure of object motion across the fingertips of a multifinger robotic hand. This can be used to estimate trends in pullout force, indicating that these signals may be useful in the feedback control of dexterous manipulation. We suspect that this is especially true for soft and underactuated robotic hands where the motions of the fingers are more influenced by external forces as compared with rigid grippers.

The RNN model is particularly susceptible to error at the beginning of the pulling trials, because suction engagement may remain relatively unchanged even as external force start to ramp up, leading to early over-predictions as shown in Fig. 13(b). These results indicate that the fingertip suction flow

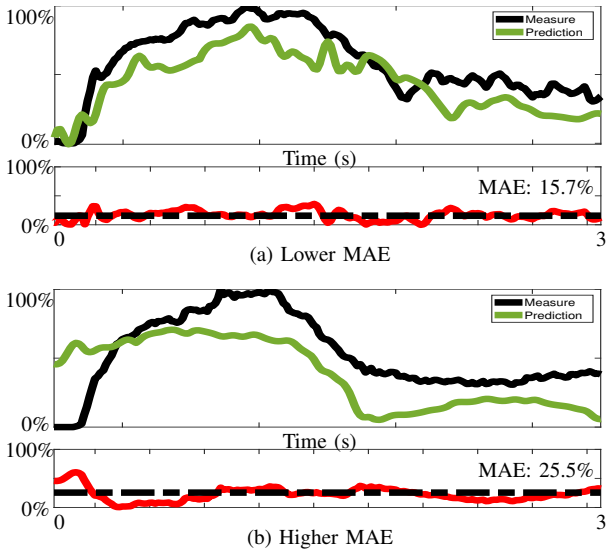

Fig. 12. Using only the suction engagement signals, a prediction of the pullout force, related to object's displacement, was generated (green) and compared to the measured force (black, solid). The absolute error (red) and its mean (black, dashed) were then computed and used to quantify the quality of the prediction.

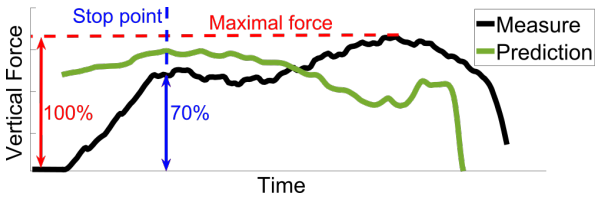

Fig. 13. A "stop point" metric is calculated as the moment where the predicted reaction forces reaches its maximum. The performance metric for one trial is defined as the measured force at the stop point, as a percentage of the maximum measured force. This example is evaluated at 70%.

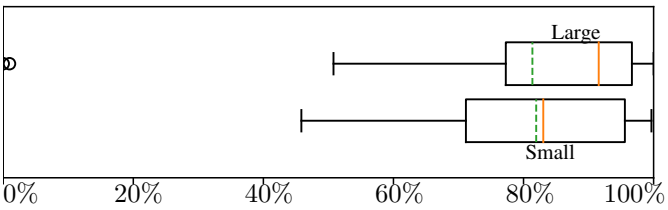

Fig. 14. Maximal force prediction performance and distribution for both data sets: continuous pulls with the large tube and discontinuous pulling with the small tube. The mean (green, dashed vertical line) of the results are 81% and 82% respectively. The median (orange, solid vertical line) are 92% and 83% respectively. Whiskers have a maximal length of 1.5 times the interquartile range.

sensing modality should be paired with complementary data, such as robot manipulator motion, to provide more accurate predictions under varying conditions. This work specifically does not include these features in order to mitigate overfitting to our particular experimental setup. This machine learning approach should be treated as a proof-of-concept demonstration.

A. Application to robot control

During dexterous manipulation, it is useful to measure and prevent grasp failure events, such as having the object be pulled out of the hand. We study the utility of the model developed in this work by comparing the real peak pulling force with the experimental force at the time when the predicted maximum occurs. This performance metric is summarized in Fig. 13. It allows us to better understand how error in the prediction could impact robot behaviors designed only to prevent pullout grasp failures.

Applying this performance metric to the same set of trials in Fig. 11 yields the results summarized in Fig. 14. The median achieved force is 92% and 83% of the maximal force for the continuous/large and discontinuous/small trials respectively. The discontinuous/small result is especially notable since the RNN was not trained on any of the trials done with the smaller sized pipes or discontinuous pulling motion, and since the evolution of the vertical reaction force is noticeably different under these conditions, as shown in Fig. 9.

There is large variability in the outcomes, sometimes resulting in predictions that are approximately 50% of the actual force peak. Notably, there are two outliers with values around 0%. These data points are trials with high MAE and predictions characterized by peak force predictions early in the trial – failure is conservatively predicted before significant pulling forces are applied.

VII. Conclusions

Suction flow rate monitoring is a meaningful way to perform tactile sensing with an underwater, suction-enabled hand. When suction is applied to the fingertips, the flow rate signal is sensitive to subtle hand-object motions during pinching that occur during manipulation. While this sensing modality could be treated as a binary contact sensor, we find that the monitoring of the analog signal throughout a grasping maneuver can allow us to predict, and potentially prevent, grasp failures.

A. Future work

There exist several potential branches for future work. More experimentation with a variety of objects and manipulation primitives should be performed to better understand the generality of this sensing modality. The addition of more suction sensors and orifices on different locations of a multi-finger gripper will also be explored. Finally, suction tactile sensing will be fused with other complementary sensors to enhance our capacity to precisely control the fingers and arms during dexterous tasks.

Acknowledgment

Philippe Nadeau was supported by the Natural Sciences and Engineering Research Council (grant number USRA-539620-2019). Michael Abbott was supported by the National Science Foundation Graduate Research Fellowship Program (award number DGE 1752814). The authors acknowledge the support of Vincent Duchaine, Mark Cutkosky and the members of the Embodied Dexterity Group.

REFERENCES

[1] F. Negrello, H. S. Stuart, and M. G. Catalano, "Hands in the real world," *Frontiers in Robotics and AI*, vol. 6, p. 147, 2020.

[2] M. L'Hour and V. Creuze, *French Archaeology's Long March to the Deep—The Lune Project: Building the Underwater Archaeology of the Future*, 01 2016, vol. 109, pp. 911–927.

[3] L. Birglen, T. Laliberté, and C. M. Gosselin, *Underactuated robotic hands*. Springer, 2007, vol. 40.

[4] G. A. Kragten and J. L. Herder, "The ability of underactuated hands to grasp and hold objects," *Mechanism and Machine Theory*, vol. 45, no. 3, pp. 408–425, 2010.

[5] R. Deimel and O. Brock, "Soft hands for reliable grasping strategies," in *Soft Robotics*. Springer, 2015, pp. 211–221.

[6] A. M. Dollar and R. D. Howe, "Joint coupling design of underactuated hands for unstructured environments," *The International Journal of Robotics Research*, vol. 30, no. 9, pp. 1157–1169, 2011.

[7] K. C. Galloway, K. P. Becker, B. Phillips, J. Kirby, S. Licht, D. Tchernov, R. J. Wood, and D. F. Gruber, "Soft robotic grippers for biological sampling on deep reefs," *Soft Robotics*, vol. 3, no. 1, pp. 23–33, 2016.

[8] H. Stuart, S. Wang, O. Khatib, and M. R. Cutkosky, "The ocean one hands: An adaptive design for robust marine manipulation," *The International Journal of Robotics Research*, vol. 36, no. 2, pp. 150–166, 2017.

[9] D. M. Lane, J. B. C. Davies, G. Robinson, D. J. O'Brien, J. Sneddon, E. Seaton, and A. Elfstrom, "The AMADEUS dextrous subsea hand: design, modeling, and sensor processing," *IEEE Journal of Oceanic Engineering*, vol. 24, no. 1, pp. 96–111, 1999.

[10] J. Lemburg, P. Kampmann, and F. Kirchner, "A small-scale actuator with passive-compliance for a fine-manipulation deep-sea manipulator," in *Proceedings of OCEANS MTS/IEEE*, 2011, pp. 1–4.

[11] M. S. Li, R. van der Zande, A. Hernandez-Agreda, P. Bongaerts, and H. S. Stuart, "Gripper design with rotation-constrained teeth for mobile manipulation of hard, plating corals with human-portable rovs," in *Proceedings of the OCEANS MTS/IEEE*, 2019.

[12] Schilling Robotics LLC, "Manipulator systems," April 2019. [Online]. Available: https://www.technipfmc.com/en/what-we-do/subsea/Robotics/manipulator-systems

[13] N. R. Sinatra, C. B. Teeple, D. M. Vogt, K. K. Parker, D. F. Gruber, and R. J. Wood, "Ultragentle manipulation of delicate structures using a soft robotic gripper," *Science Robotics*, vol. 4, no. 33, p. eaax5425, 2019.

[14] K. A. Walker, A. W. Trites, M. Haulena, and D. M. Weary, "A review of the effects of different marking and tagging techniques on marine mammals," *Wildlife Research*, vol. 39, no. 1, pp. 15–30, 2012.

[15] N. C. Dobson, "Developmental deep-water archaeology: a preliminary report on the investigation and excavation of the 19th-century side-wheel steamer ss republic, lost in a storm off savannah in 1865," in *Proceedings of the OCEANS MTS/IEEE*. IEEE, 2005, pp. 1761–1769.

[16] H. S. Stuart, S. Wang, and M. R. Cutkosky, "Tunable contact conditions and grasp hydrodynamics using gentle fingertip suction," *IEEE Transactions on Robotics*, vol. 35, no. 2, pp. 295–306, 2018.

[17] H. Yousef, M. Boukallel, and K. Althoefer, "Tactile sensing for dexterous in-hand manipulation in robotics—a review," *Sensors and Actuators A: physical*, vol. 167, no. 2, pp. 171–187, 2011.

[18] Z. Kappassov, J.-A. Corrales, and V. Perdereau, "Tactile sensing in dexterous robot hands," *Robotics and Autonomous Systems*, vol. 74, pp. 195–220, 2015.

[19] M. R. Cutkosky and W. Provancher, "Force and tactile sensing," in *Springer Handbook of Robotics*. Springer, 2016, pp. 717–736.

[20] J. Dennerlein, R. Howe, E. Shahoian, and C. Olroyd, "Vibrotactile feedback for an underwater telerobot," in *Robotics and applications; Robotic and manufacturing systems recent results in research, development and applications International symposium*. Citeseer, 2000, pp. 244–249.

[21] P. Kampmann and F. Kirchner, "A tactile sensing system for underwater manipulation," in *Proceedings of the 7th ACM/IEEE International Conference on Human-Robot Interaction*. IEEE, 2012.

[22] A. Aggarwal, P. Kampmann, J. Lemburg, and F. Kirchner, "Haptic object recognition in underwater and deep-sea environments," *Journal of field robotics*, vol. 32, no. 1, pp. 167–185, 2015.

[23] S. Moe, K. Schjølberg-Henriksen, D. Wang, E. Lund, J. Nysæther, L. Furuberg, M. Visser, T. Fallet, and R. Bernstein, "Capacitive differential pressure sensor for harsh environments," *Sensors and Actuators A: Physical*, vol. 83, no. 1-3, pp. 30–33, 2000.

[24] P. J. Sanz, A. Penalver, J. Sales, D. Fornas, J. J. Fernández, J. Pérez, and J. Bernabé, "Grasper: A multisensory based manipulation system for underwater operations," in *Proceedings of the IEEE International Conference on Systems, Man, and Cybernetics*. IEEE, 2013, pp. 4036–4041.

[25] H. S. Stuart, M. Bagheri, S. Wang, H. Barnard, A. L. Sheng, M. Jenkins, and M. R. Cutkosky, "Suction helps in a pinch: Improving underwater manipulation with gentle suction flow," in *Proceedings of the IEEE/RSJ international conference on intelligent robots and systems (IROS)*. IEEE, 2015, pp. 2279–2284.

[26] K. Yamaguchi, Y. Hirata, and K. Kosuge, "Development of robot hand with suction mechanism for robust and dexterous grasping," in *Proceedings of the IEEE/RSJ International Conference on Intelligent Robots and Systems*. IEEE, 2013, pp. 5500–5505.

[27] N. Correll, K. E. Bekris, D. Berenson, O. Brock, A. Causo, K. Hauser, K. Okada, A. Rodriguez, J. M. Romano, and P. R. Wurman, "Analysis and observations from the first amazon picking challenge," *IEEE Transactions on Automation Science and Engineering*, 2016.

[28] M. Schwarz, C. Lenz, G. M. García, S. Koo, A. S. Periyasamy, M. Schreiber, and S. Behnke, "Fast object learning and dual-arm coordination for cluttered stowing, picking, and packing," in *Proceedings of the IEEE International Conference on Robotics and Automation (ICRA)*. IEEE, 2018, pp. 3347–3354.

[29] D. Morrison, A. W. Tow, M. McTaggart, R. Smith, N. Kelly-Boxall, S. Wade-McCue, J. Erskine, R. Grinover, A. Gurman, T. Hunn *et al.*, "Cartman: The low-cost cartesian manipulator that won the amazon robotics challenge," in *Proceedings of the IEEE International Conference on Robotics and Automation (ICRA)*. IEEE, 2018, pp. 7757–7764.

[30] H. Zhang, J. Zhang, G. Zong, W. Wang, and R. Liu, "Sky cleaner 3: A real pneumatic climbing robot for glass-wall cleaning," *IEEE Robotics & Automation Magazine*, vol. 13, no. 1, pp. 32–41, 2006.

[31] G. La Rosa, M. Messina, G. Muscato, and R. Sinatra, "A low-cost lightweight climbing robot for the inspection of vertical surfaces," *Mechatronics*, vol. 12, no. 1, pp. 71–96, 2002.

[32] S. Siami-Namini, N. Tavakoli, and A. S. Namin, "A comparison of arima and lstm in forecasting time series," in *Proceedings of the 17th IEEE International Conference on Machine Learning and Applications (ICMLA)*. IEEE, 2018, pp. 1394–1401.

[33] H. Shi, M. Xu, and R. Li, "Deep learning for household load forecasting—a novel pooling deep rnn," *IEEE Transactions on Smart Grid*, vol. 9, no. 5, pp. 5271–5280, 2017.

[34] F. Chollet *et al.*, "Keras," https://keras.io, 2015.

[35] M. Abadi, A. Agarwal, P. Barham, E. Brevdo, Z. Chen, C. Citro, G. S. Corrado, A. Davis, J. Dean, M. Devin, S. Ghemawat, I. Goodfellow, A. Harp, G. Irving, M. Isard, Y. Jia, R. Jozefowicz, L. Kaiser, M. Kudlur, J. Levenberg, D. Mané, R. Monga, S. Moore, D. Murray, C. Olah, M. Schuster, J. Shlens, B. Steiner, I. Sutskever, K. Talwar, P. Tucker, V. Vanhoucke, V. Vasudevan, F. Viégas, O. Vinyals, P. Warden, M. Wattenberg, M. Wicke, Y. Yu, and X. Zheng, "TensorFlow: Large-scale machine learning on heterogeneous systems," 2015, software available from tensorflow.org. [Online]. Available: https://www.tensorflow.org/

[36] D. P. Kingma and J. Ba, "Adam: A method for stochastic optimization," *arXiv preprint arXiv:1412.6980*, 2014.